Applied Physics Letters ARTICLE scitation.org/journal/apl

Valley polarized conductance quantization in bilayer graphene narrow quantum point contact

Cite as: Appl. Phys. Lett. **118**, 263102 (2021); doi: 10.1063/5.0052845
Submitted: 1 April 2021 · Accepted: 30 May 2021 ·
Published Online: 30 June 2021

Kohei Sakanashi,[1,a)] Naoto Wada,[1] Kentaro Murase,[1] Kenichi Oto,[2] Gil-Ho Kim,[3] Kenji Watanabe,[4] Takashi Taniguchi,[5] Jonathan P. Bird,[6] David K. Ferry,[7] and Nobuyuki Aoki[1,a)]

AFFILIATIONS

[1]Department of Materials Science, Chiba University, Chiba 263-8522, Japan
[2]Department of Physics, Chiba University, Chiba 263-8522, Japan
[3]School of Electronic and Electrical Engineering and Sungkyunkwan Advanced Institute of Nanotechnology (SAINT), Sungkyunkwan University (SKKU), Suwon 16419, South Korea
[4]International Centre for Materials Nanoarchitectonics, National Institute for Materials Science, 1-1 Namiki, Tsukuba 305-0044, Japan
[5]Research Centre for Functional Materials, National Institute for Materials Science, 1-1 Namiki, Tsukuba 305-0044, Japan
[6]Department of Electrical Engineering, University at Buffalo, The State University of New York, Buffalo, New York 14260, USA
[7]School of Electrical, Computer, and Energy Engineering, Arizona State University, Tempe, Arizona 85287-5706, USA

[a)]Authors to whom correspondence should be addressed: k.sakanashi@chiba-u.jp and n-aoki@faculty.chiba-u.jp

ABSTRACT

In this study, we fabricated quantum point contacts narrower than 100 nm by using an electrostatic potential to open the finite bandgap by applying a perpendicular electric field to bilayer graphene encapsulated between hexagonal boron nitride sheets. The conductance across the quantum point contact was quantized at a high perpendicular-displacement field as high as 1 V/nm at low temperature, and the quantization unit was $2e^2/h$ instead of mixed spin and valley degeneracy of $4e^2/h$. This lifted degeneracy state in the quantum point contact indicates the presence of valley polarized state coming from potential profile or effective displacement field in one-dimensional channel.

Published under an exclusive license by AIP Publishing. https://doi.org/10.1063/5.0052845

A short one-dimensional channel, namely, a quantum point contact (QPC), defined in two-dimensional materials has been receiving much attention for future spin-valley device applications such as a spin-valley filter or spin-valve effect.[1,2] Several QPC devices have already been realized in two-dimensional materials such as electrostatically induced bilayer graphene (BLG),[3–10] etching-defined monolayer graphene,[11–14] or transitional metal dichalcogenide.[15–17] However, the phenomena attributed to degrees of freedom, such as valley and spin in the QPC, are still unclear and controversial.

Monolayer graphene, which has Dirac dispersion, is not applicable for electrostatically confined nanostructures such as the QPC due to its lack of an energy gap;[18] therefore, an etching-defined QPC structure was used, which is also used in conventional high-electron mobility transistor systems in several ways.[11,14] Such graphene QPC devices show strong disorder and inhomogeneity effects, consequently causing inter-valley scattering,[19] localized state effects,[20] or low transmission probability.[19] Even bilayer graphene has no energy gap in the intrinsic situation; however, a bandgap can open with a perpendicular electric field.[21,22] Then, electrically confined nanostructures can be realized in BLG by fabricating sandwiched structure with top and bottom metallic gates.[3–10] However, in order to form a bandgap sufficient for defining the QPC in the BLG, a relatively high displacement field ($>$ 0.3 V/nm) is necessary by applying opposite-polarity voltages between the top (bottom) split gates and the global back (top) gate,[21–23] and then the carrier density in the two-dimensional electron (hole) gas region (2DEG or 2DHG), except underneath the split gates, becomes high—up to the order of a few 10^{12} cm^{-2} causing lower mobility. Forming a well-defined QPC channel electrostatically requires an adequate high displacement field inside the QPC channel that runs between the split gates. However, BLG has a relatively short Fermi wavelength compared to a conventional HEMT system,[18] and an even shorter channel width between the split gates ($<$ 50 nm), so it is difficult to pinch-off the current channel because of the fringing effect of the electric field at the edge of the split gates.[9] To achieve the pinch-off properties and well tunability of Fermi wavelength in the QPC channel, a triple-gate (a channel-gate) structure, which has an additional high-k dielectric,

Published under an exclusive license by AIP Publishing

and a top gate were utilized, and then clear quantized conductance steps were observed in units of $4e^2/h$.[3,4,7,8] In these structures, the QPC channel width is typically 150–250 nm, and the pinch-off can be achieved with depleting the carriers in the channel by applying an appropriate voltage to the channel gate without squeezing the channel width. Then, the conductance steps usually appear at every $4e^2/h$. However, the value of the steps sometimes appears at $2e^2/h$ depending on samples. So the unit of the conductance quantization is not a unique value and is still unclear.[3] In this paper, we realized split-gate structures less than 100 nm and studied the transport properties by changing the confinement potential profile by changing the voltage applying to the split gates.

In this paper, we mainly measured two types of devices, named device A [Figs. 1(a) and 1(b)] and device B [Figs. 1(c) and 1(d)]. All BLG flakes and hexagonal boron nitride (hBN) crystals used for the two devices were exfoliated onto SiO_2/Si chips from bulk crystals and carefully chosen by means of optical microscopy, Raman spectroscopy, and atomic force microscopy (AFM) to ensure the thickness and cleanness. A stack of a hBN/BLG/hBN heterostructure was assembled by PC (6% Poly bisphenol A Carbonate dissolved in chloroform)/PDMS based dry-transfer method[24] and released on the top of the cleaned 300 nm-thick SiO_2 layer on the p^{++}-Si substrate working as a global back gate (BG) for device A. The split gate electrodes (SG) for QPC1 were fabricated on the stack at the final step as schematically shown in Fig. 1(b). For device B, prior to attaching the stack, the thin metallic SG electrodes for the QPC2 were fabricated on the SiO_2 surface, and the top gate covering the QPC2 and 2DEG (2DHG) region was fabricated on the stack as shown in Fig. 1(d). The Si substrate was also used to control the perpendicular electric field. All the electrodes were fabricated by means of electron beam lithography (EBL) and electron beam deposition (EBD) of Cr 1/AuPd 9 nm. The channel region was patterned by standard EBL, followed by reactive ion etching (RIE) in a gas mixture of CHF_3 (10) and O_2 (4.5 sccm) in a home-built etcher at 60 W. Source-drain electrodes were formed by the one dimensional edge contact technique[24] through the EBL, RIE, and EBD (Cr 3/Pd 15/Au 80 nm) with the same PMMA mask to avoid contamination and any self-bias effect.[25] We record typical series resistance of a few hundreds to kΩ in our devices. All of the SG have the same dimension of 100 nm-wide and 100-nm-long at the top with a triangular shape, and the coarse part has a 1-μm-width as shown in the inset of Fig. 1(a). All electrical measurements were measured by standard lock-in techniques at the frequency of the 17.7 Hz with a small excitation voltage, below 100 μV, in four terminal configurations for device A and two terminals for device B at low temperature in a JANIS ^{3}He refrigerator. During the measurement, QPC1 in device A was defined by applying positive and negative gate voltages to the SG and the BG, respectively, in order to apply a perpendicular electric field. In the device B, the QPC2 was defined in the same manner; however, the global BG was biased in the same polarity to the SG in order to assist the perpendicular electric field within the conducting 1D channel and to decrease the carrier density in the 2DEG (2DHG) region for increasing the mobility.

Figure 1(e) shows a resistance curve of device A as a function of the back-gate voltage (V_{BG}) at 2 K. The highest field-effect carrier mobility was 57 000 cm^2/V s. Figure 1(f) shows a resistance curve of device B as a function of the global top-gate voltage (V_{TG}) at 2 K. The residual impurity density in device A is below 10^{11} cm^{-2} (see the supplementary material Fig. S1). This high-quality BLG device has a longer mean free path than the width and the length of the split gates. The resistance map of the V_{BG} and the top split gate voltage (V_{SG}) sweeps shows higher resistance peeks at around $V_{BG} = -3$ V for the Dirac point of the BLG and at along the slope upward to the left related to the higher displacement field, D, comparable with earlier studies,[3,9] where $D = (D_{top} + D_{bottom})/2$ where $D_{top} = -\varepsilon_{top}(V_{sg} - V_{CNP})/d_{top}$ and $D_{bottom} = \varepsilon_{bottom}(V_{bg} - V_{CNP})/d_{bottom}$[21,22] (see the supplementary material Fig. S2). Each ε and d are determined by using

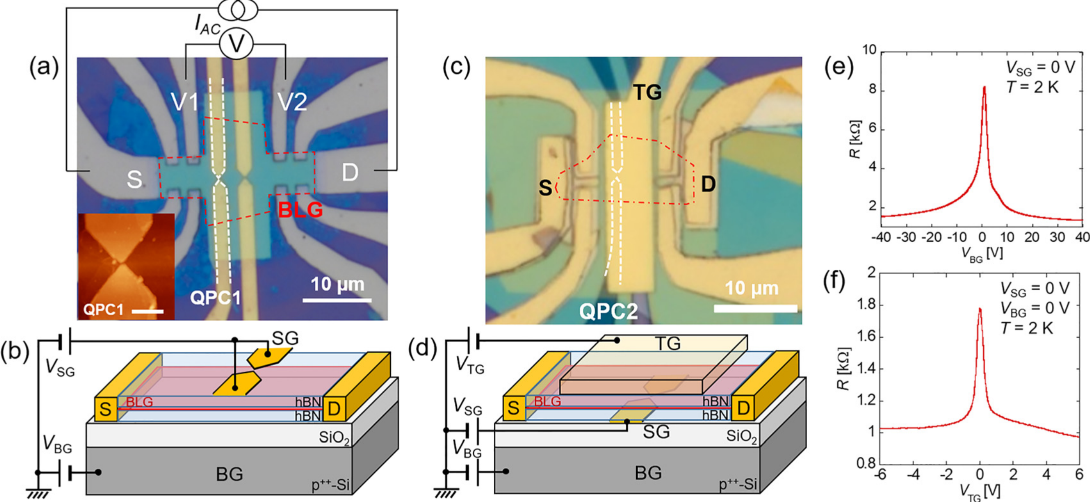

FIG. 1. (a) Optical microscope image and (b) schematic view of the device A. Red dotted line indicates the position of the BLG flake embedded in the hBN layers. The inset in (a) shows AFM image of the tip of the SG. The scale bar is 500 nm. (c) Optical microscope image and (d) schematic view of the device B. White dotted lines indicates the position the QPC2 underneath the hBN/BLG/hBN stack. (e) V_{BG} dependence of the two-terminal resistance of device A at 2 K. (f) V_{TG} dependence of the two-terminal resistance of the device B at 2 K. All other gates were grounded during the mesurements.

Published under an exclusive license by AIP Publishing

the dielectric constant and the thickness of the dielectric layers, respectively. When the $|D|$ exceeds 1 V/nm, the BLG underneath the SGs can open a certain level of bandgap at the Dirac point, and the charge is depleted enough to define the QPC.[21] Figure 2(a) shows a typical transfer curve by sweeping the V_{SG} toward the positive voltage by applying fixed $V_{BG} = -80$ V. The conductance decreased slowly at $0 < V_{SG} < 4$ V due to the formation of p^+pp^+ junction (regime I) since high hole density in 2DHG was induced by negatively biasing the global back gate electrode and the carrier density underneath the SGs was slightly decreased. In the middle displacement field regime, the 2DHG under SGs was getting depleted by approaching the Dirac point, and the conductance starts to decrease drastically (regime II). Under a high displacement field region, $|D| \sim 1$ V/nm, a sufficient bandgap was formed at the Dirac point in the BLG underneath the SG electrodes (see the supplementary material Fig. S3). The 2DHG in the region was depleted since the Fermi level of BLG was tuned to the middle of bandgap, and then a QPC structure was electrostatically defined. The conducting channel was getting squeezed, and quantized plateaus appeared in the conductance curve (regime III) are magnified in Fig. 2(b). After exceeding the critical V_{SG} value of around $V_{SG} = 9.3$ V, the conductance increases again (regime IV) by the Fermi level reaching the conduction band edge underneath the SG and conduction begins to revive by forming a p^+np^+ junction due to Klein tunneling.[26] Note that both carrier density and displacement field strength in the constriction are changed during the single V_{SG} sweeping. The quantization of the conductance is unclear compared to such QPCs in a conventional semiconductor heterostructure due to the shorter mean free path in this system and the geometrical shape of the SG electrodes. Nevertheless, the derivative of conductance with respect to V_{SG} shows well-developed maxima corresponding to the position of the plateaus at steps of $2e^2/h$ covering a wide range of conductance, where the derivative of conductance is usually negative due to the p-type QPC as shown in Fig. 2(b). However, the conductance did not go below $2 \times 2e^2/h$ in this sample even by increasing the negative back gate voltage up to -110 V (see the supplementary material Fig. S2). The reasons why the QPC did not reach a pinch-off could be considered as follows: The QPC can be defined only during the V_{SG} range when the Fermi level under the SG is in the bandgap (see the supplementary material Fig. S3); therefore, only a finite number of conductance steps (five steps in this case) can be observed within the energy (gate voltage) window. Since the carrier density in the 2DHG region is rather high, up to 5×10^{12} cm^{-2}, due to the large back gate voltage (>-80 V) to induce sufficient displacement field to open the bandgap under the SGs, the stray field from the tip of the SG into the QPC channel is not sufficient to deplete the carrier density completely in the channel. Moreover, in order to achieve the pinch-off condition in the QPC, a perpendicular electric field is necessary to open a sufficient bandgap in the channel region. However, it is not sufficient only from the tip of the SGs even using a narrow separation less than 100 nm. Another set of gate electrodes provide such a channel gate[3–5,7,8] to assist the perpendicular electric field to achieve the pinch-off.

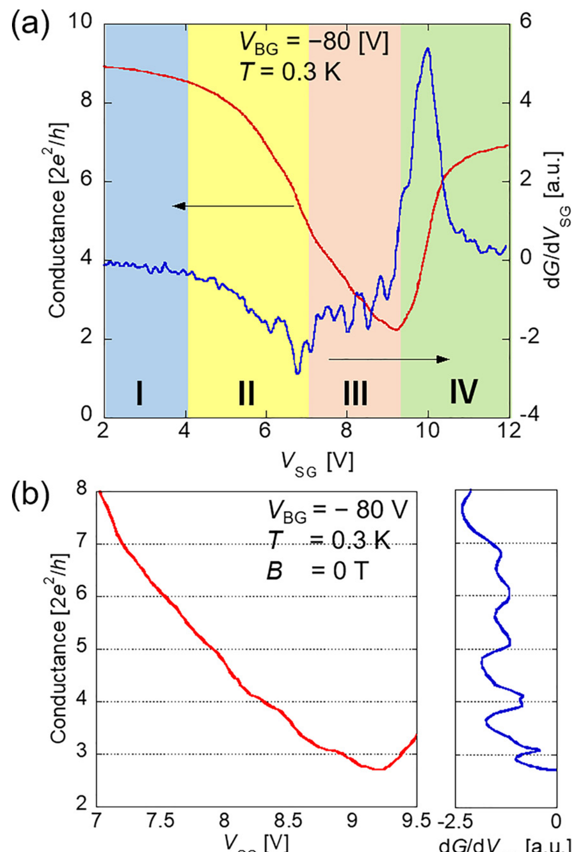

FIG. 2. (a) Conductance (red) and its derivative (blue) with respect to V_{SG} (dG/dV_{SG}) of QPC1 in device A, obtained by sweeping V_{SG} at $V_{BG} = -80$ V. The background color indicates the different transport regimes (I–IV). (b) Left panel: conductance curve at regime III in (a) after subtraction of series resistance. Right panel: differential conductance (dG/dV_{SG}) of the curve in the left panel.

Nevertheless, our results exhibit a feature of the level degeneracy of quantized conductance with a unit of $2e^2/h$ after subtraction of series resistance ($R_{series} \sim 1$ kΩ) of the 2DHG region from the measured 4-t resistance (R_{4t}), $G_{QPC} = 1/(R_{4t} - R_{series})$ in e^2/h unit formula shown in Fig. 2(b). Due to zero magnetic field and relatively small spin–orbit coupling in the BLG system, such a BLG-QPC should show the quantization units of $g = 4$ for the valley (2) and the spin degeneracy (2). Our results suggest a possibility of breaking the valley degeneracy in the narrow constriction. The quantization unit can be modified by transmission probability T when the constriction geometry is not uniform or quantum wire case instead of QPC geometry. However, the transmission probability would not be restricted so much from $T \sim 1$ since the length of the QPC (100) is sufficiently shorter than the mean free path ($\sim$500 nm), estimated from the field-effect mobility (57 000 cm^2/V s) near the Dirac point. Another possibility is intervalley scattering due to the scattering at atomic defects, sample edge roughness, or variations in the etching defined hard-wall potential. However, our electrostatically induced soft-wall and smooth confinement potential, which has no dissipative edge or roughness, should show the transparency $T \sim 1$. Similar studies have been performed using electrostatically induced QPCs and quantum wires in BLG, where they have reported quantized conductance steps of $4e^2/h$. The main differences of these former studies from our device are the use of a wide channel more than 200 nm and an additional channel gate structure in order to assist the perpendicular electric field to achieve

Published under an exclusive license by AIP Publishing

the pinch-off condition.[3–5,7] On the other hand, such QPC structures having a narrow constriction width less than 100 nm (similar to our devices) tend to show $g = 2$,[9,10] whose QPCs are used for defining a quantum dot. Considering the differences of the channel width, the landscapes of the confinement potential would be different; a rectangular potential profile could be considered for the wide channel and then the additional channel gate decreased carrier density and increased the Fermi wavelength to achieve the mode at the discrete energy level. On the other hand, the narrow constriction, less than 100 nm, used in QPC1, provides a parabolic-soft-wall potential and then the degeneracy may be removed by the confinement effect. By applying an out-of-plane magnetic field, the one-dimensional discrete energy levels split and cross each other due to the formation and the evolution of Landau levels at low magnetic field;[3,5,7] therefore, the conductance steps do not appear regularly compared to the results of in-plain magnetic field application.[10] However, at higher magnetic field $B = 9$ T, the conductance steps are still slightly complicated as the unit of conductance quantization becomes e^2/h due to the Zeeman splitting over the full gate voltage range in regime III as shown in Fig. 3 (see the supplementary material Fig. S4 for the Landau fan plot from $B = 0$ to 9 T). Different from the former BLG-QPC studies using a channel gate structure,[3–5,7,8] no significant enlargement of the width of the conductance plateau is observed even at 9 T due to the channel width (< 80 nm) narrower than the cyclotron radios in our QPC device.

Such a $g = 2$ quantization behavior has also been confirmed in another BLG-QPC device, QPC2 in device B, which has a triple-gate structure shown in Figs. 1(c) and 1(d) and higher mobility. Clear conductance steps with a unit of $2e^2/h$ can be observed at $3–6 \times 2e^2/h$ after subtracting R_{series} as shown in Fig. 4. In this experiment, the $|D|$ between the top gate and the SG was 0.7 in addition to the $|D|$ of 0.7 V/nm between the top gate and the BG for the assistance of the perpendicular electric field in the 2DHG region including the channel. Although the minimum conductance decreased down to $2e^2/h$, it could not achieve the pinch-off due to the small energy window of the depletion at the SG region. Some additional small conductance steps can be observed in Fig. 4. These features may originate from quantum intereference due to disorder in the QPC region, or from Fabry–Pérot interference in the split-gate region, resulting from parallel conduction due to the presence of insufficient gate voltage.[26–30] These additional steps can be observed also due to hole-hole intereaction, although the mobility of our devices may not be sufficiently large to allow such many-body effects.[31–33]

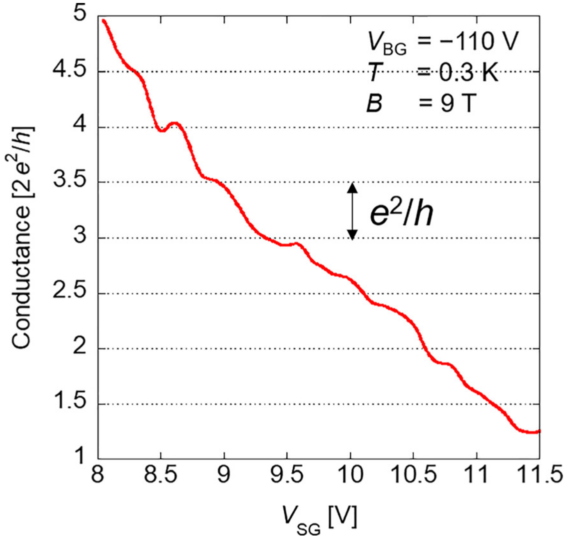

FIG. 3. Conductance of QPC1 in device A as a function of V_{SG} at $V_{BG} = -110$ V and $B = 9$ T.

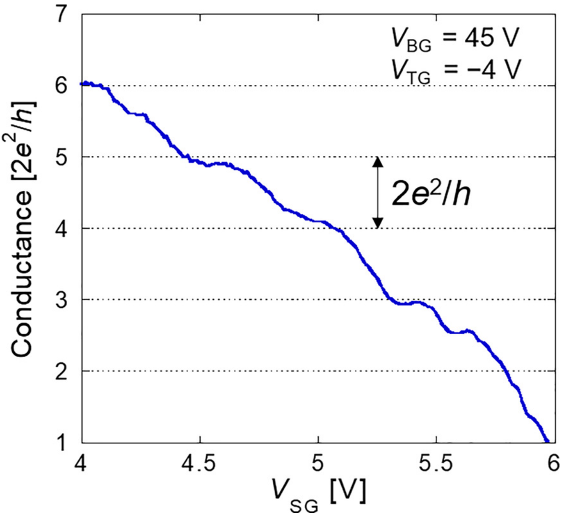

FIG. 4. Conductance of QPC2 in device B as a function of bottom split gate voltage V_{SG} at $V_{TG} = -4$ Vand $V_{BG} = 45$ V.

In summary, we have demonstrated electrostatically confined QPC structures narrower than 100 nm without the assistance of additional channel gates and observed the well-developed quantized conductance at steps of $2e^2/h$ instead of $4e^2/h$ although the conductance is not fully pinched-off. The step of $2e^2/h$ suggests the breaking of at least one degeneracy such as valley polarization by perpendicular electric fields, and these results indicate the narrow confinement potential profile may be responsible for lifting the valley degeneracy suggesting for the application as such a valley filter device.

See the supplementary material for the device quality estimation, resistance evolution in dual-gate sweep, and how to define the BLG-QPC.

The authors thank Yu Saito for fruitful discussion on device fabrication. This work was supported by the JSPS KAKENHI Grant Nos. 18H0812 and 20J20052, JSPS Bilateral Joint Research with NRF, Chiba University VBL project, and Iketani Science and Technology Foundation. The work was also supported by the National Research Foundation of Korea (NRF) grant funded by the Korea government (MSIT) with file No. 2021K2A9A2A08000168.

DATA AVAILABILITY

The data that support the findings of this study are available from the corresponding authors upon reasonable request.

Published under an exclusive license by AIP Publishing

REFERENCES

[1]A. Rycerz, J. Tworzydło, and C. W. J. Beenakker, Nat. Phys. **3**, 172 (2007).
[2]D. Xiao, W. Yao, and Q. Niu, Phys. Rev. Lett. **99**, 236809 (2007).
[3]H. Overweg, H. Eggimann, X. Chen, S. Slizovskiy, M. Eich, R. Pisoni, Y. Lee, P. Rickhaus, K. Watanabe, T. Taniguchi, V. Fal'Ko, T. Ihn, and K. Ensslin, Nano Lett. **18**, 553 (2018).
[4]H. Overweg, A. Knothe, T. Fabian, L. Linhart, P. Rickhaus, L. Wernli, K. Watanabe, T. Taniguchi, D. Sánchez, J. Burgdörfer, F. Libisch, V. I. Fal'Ko, K. Ensslin, and T. Ihn, Phys. Rev. Lett. **121**, 257702 (2018).
[5]L. Banszerus, B. Frohn, T. Fabian, S. Somanchi, A. Epping, M. Müller, D. Neumaier, K. Watanabe, T. Taniguchi, F. Libisch, B. Beschoten, F. Hassler, and C. Stampfer, Phys. Rev. Lett. **124**, 177701 (2020).
[6]M. Kim, J. H. Choi, S. H. Lee, K. Watanabe, T. Taniguchi, S. H. Jhi, and H. J. Lee, Nat. Phys. **12**, 1022 (2016).
[7]Y. Lee, A. Knothe, H. Overweg, M. Eich, C. Gold, A. Kurzmann, V. Klasovika, T. Taniguchi, K. Wantanabe, V. Fal'Ko, T. Ihn, K. Ensslin, and P. Rickhaus, Phys. Rev. Lett. **124**, 126802 (2020).
[8]R. Kraft, I. V. Krainov, V. Gall, A. P. Dmitriev, R. Krupke, I. V. Gornyi, and R. Danneau, Phys. Rev. Lett. **121**, 257703 (2018).
[9]A. M. Goossens, S. C. M. Driessen, T. A. Baart, K. Watanabe, T. Taniguchi, and L. M. K. Vandersypen, Nano Lett. **12**, 4656 (2012).
[10]M. T. Allen, J. Martin, and A. Yacoby, Nat. Commun. **3**, 934 (2012).
[11]N. Tombros, A. Veligura, J. Junesch, M. H. D. Guimarães, I. J. Vera-Marun, H. T. Jonkman, and B. J. Van Wees, Nat. Phys. **7**, 697 (2011).
[12]V. Clericò, J. A. Delgado-Notario, M. Saiz-Bretín, A. V. Malyshev, Y. M. Meziani, P. Hidalgo, B. Méndez, M. Amado, F. Domínguez-Adame, and E. Diez, Sci. Rep. **9**, 13572 (2019).
[13]S. Somanchi, B. Terrés, J. Peiro, M. Staggenborg, K. Watanabe, T. Taniguchi, B. Beschoten, and C. Stampfer, Ann. Phys. **529**, 1700082 (2017).
[14]B. Terrés, L. A. Chizhova, F. Libisch, J. Peiro, D. Jörger, S. Engels, A. Girschik, K. Watanabe, T. Taniguchi, S. V. Rotkin, J. Burgdörfer, and C. Stampfer, Nat. Commun. **7**, 11528 (2016).
[15]R. Pisoni, Y. Lee, H. Overweg, M. Eich, P. Simonet, K. Watanabe, T. Taniguchi, R. Gorbachev, T. Ihn, and K. Ensslin, Nano Lett. **17**, 5008 (2017).
[16]K. Marinov, A. Avsar, K. Watanabe, T. Taniguchi, and A. Kis, Nat. Commun. **8**, 1938 (2017).
[17]K. Wang, K. De Greve, L. A. Jauregui, A. Sushko, A. High, Y. Zhou, G. Scuri, T. Taniguchi, K. Watanabe, M. D. Lukin, H. Park, and P. Kim, Nat. Nanotechnol. **13**, 128 (2018).
[18]S. D. Sarma, S. Adam, E. H. Hwang, and E. Rossi, Rev. Mod. Phys. **83**, 407 (2011).
[19]H. Lee, G. H. Park, J. Park, G. H. Lee, K. Watanabe, T. Taniguchi, and H. J. Lee, Nano Lett. **18**, 5961 (2018).
[20]A. Epping, C. Volk, F. Buckstegge, K. Watanabe, T. Taniguchi, and C. Stampfer, Phys. Status Solidi **256**, 1900269 (2019).
[21]Y. Zhang, T. T. Tang, C. Girit, Z. Hao, M. C. Martin, A. Zettl, M. F. Crommie, Y. R. Shen, and F. Wang, Nature **459**, 820 (2009).
[22]T. Taychatanapat and P. Jarillo-Herrero, Phys. Rev. Lett. **105**, 166601 (2010).
[23]M. Eich, R. Pisoni, H. Overweg, A. Kurzmann, Y. Lee, P. Rickhaus, T. Ihn, K. Ensslin, F. Herman, M. Sigrist, K. Watanabe, and T. Taniguchi, Phys. Rev. X **8**, 031023 (2018).
[24]L. Wang, I. Meric, P. Y. Huang, Q. Gao, Y. Gao, H. Tran, T. Taniguchi, K. Watanabe, L. M. Campos, D. A. Muller, J. Guo, P. Kim, J. Hone, K. L. Shepard, and C. R. Dean, Science **342**, 614 (2013).
[25]M. B. Shalom, M. J. Zhu, V. I. Fal'ko, A. Mishchenko, A. V. Kretinin, K. S. Novoselov, C. R. Woods, K. Watanabe, T. Taniguchi, A. K. Geim, and J. R. Prance, Nat. Phys. **12**, 318 (2016).
[26]H. Overweg, H. Eggimann, M. H. Liu, A. Varlet, M. Eich, P. Simonet, Y. Lee, K. Watanabe, T. Taniguchi, K. Richter, V. I. Fal'ko, K. Ensslin, and T. Ihn, Nano Lett. **17**, 2852 (2017).
[27]A. Varlet, M. H. Liu, V. Krueckl, D. Bischoff, P. Simonet, K. Watanabe, T. Taniguchi, K. Richter, K. Ensslin, and T. Ihn, Phys. Rev. Lett. **113**, 116601 (2014).
[28]K. Zimmermann, A. Jordan, F. Gay, K. Watanabe, T. Taniguchi, Z. Han, V. Bouchiat, H. Sellier, and B. Sacépé, Nat. Commun. **8**, 14983 (2017).
[29]C. Déprez, L. Veyrat, H. Vignaud, G. Nayak, K. Watanabe, T. Taniguchi, F. Gay, H. Sellier, and B. Sacépé, Nat. Nanotechnol. **16**, 555 (2021).
[30]Y. Ronen, T. Werkmeister, D. Haie Najafabadi, A. T. Pierce, L. E. Anderson, Y. J. Shin, S. Y. Lee, Y. H. Lee, B. Johnson, K. Watanabe, T. Taniguchi, A. Yacoby, and P. Kim, Nat. Nanotechnol. **16**, 563 (2021).
[31]D. Terasawa, S. Norimoto, T. Arakawa, M. Ferrier, A. Fukuda, K. Kobayashi, and Y. Hirayama, J. Phys. Soc. Jpn. **90**, 024709 (2021).
[32]K. J. Thomas, J. T. Nicholls, M. Y. Simmons, M. Pepper, D. R. Mace, and D. A. Ritchie, Phys. Rev. Lett. **77**, 135 (1996).
[33]A. Srinivasan, D. S. Miserev, K. L. Hudson, O. Klochan, K. Muraki, Y. Hirayama, D. Reuter, A. D. Wieck, O. P. Sushkov, and A. R. Hamilton, Phys. Rev. Lett. **118**, 146801 (2017).

Published under an exclusive license by AIP Publishing